Nano World Journal

https://doi.org/10.17756/nwj.2023-s2-068

Research Article

Open Access

Optimization of Adsorption Parameters for Effective Removal of Basic Yellow Dye 28 from Aqueous Solution by Apatites Using a Factorial Design

Omar Boukra[1], Ali Boukra[1], Sanaâ Saoiabi[1*], Souhayla Latifi[1,2], Youssef Khallouki[1], Anas Krime[1], Soumia Berrahou[1], Larbi El Hammari[1] and Ahmed Saoiabi[1]

[1]*Laboratory of Applied Chemistry of Materials, Department of Chemistry, Faculty of Sciences, Mohammed V University, Rabat, Morocco*

[2]*Laboratory REMTEX, ESITH (Higher School of Textile and Clothing Industries), Casablanca, Morocco*

[*]Correspondence to:
Sanaâ Saoiabi
Laboratory of Applied Chemistry of Materials, Department of Chemistry, Faculty of Sciences, Mohammed V University, Rabat, Morocco.
E-mail: s.saoiabi@yahoo.com

Received: July 25, 2023
Accepted: September 26, 2023
Published: September 29, 2023

Citation: Boukra O, Boukra A, Saoiabi S, Latifi S, Khallouki Y, et al. 2023. Optimization of Adsorption Parameters for Effective Removal of Basic Yellow Dye 28 from Aqueous Solution by Apatites Using a Factorial Design. *NanoWorld J* 9(S2): S401-S407.

Copyright: : © 2023 Boukra et al. This is an Open Access article distributed under the terms of the Creative Commons Attribution 4.0 International License (CCBY) (http://creativecommons.org/licenses/by/4.0/) which permits commercial use, including reproduction, adaptation, and distribution of the article provided the original author and source are credited.

Published by United Scientific Group

Abstract

This study focuses on the potential use of apatitic materials grafted with aminotrimethylene phosphonic acid (HAp-AMP) at different grafting rates (0%, 2.5%, 5%, and 10%) as basic yellow dye adsorbents 28. These apatitic materials were prepared by a precipitation process at 25 °C in an aqueous medium according to the rapid neutralization of calcium hydroxide ($Ca(OH)_2$) by ammonium dihydrogen phosphate ($NH_4H_2PO_4$). The synthesized materials were characterized by various analytical techniques to determine physicochemical properties such as XRD, FTIR, BET, respectively. Design-of-experiments study of the adsorption process of basic yellow dye 28 on the synthesized powder with the highest adsorbed dye content. For this we chose the material (HAp-AMP 10%) as a representative model. This study was carried out by applying a factorial design using Design-Expert software to distinguish among three factors (concentrations of basic yellow 28, contact time between adsorbent and adsorbate, and pH) those currently considered to be potentially influential. The results show that the adsorption capacity of adsorbent towards the cationic dye was 31.38 mg/g obtained at 298 K with an initial concentration of 75 mg/L, a contact time of 67 min and while pH had no significant impact on adsorption compared to the other parameters.

Keywords

Pollution, Basic yellow 28, Hydroxyapatite, Aminotrimethylene phosphonic acid, Adsorption, Optimization

Abbreviations

HAp: Hydroxyapatite; AMP: Aminotrimethylene phosphonic acid; HAp-AMP: Hydroxyapatite grafted by aminotrimethylene phosphonic acid; XRD: X-ray diffraction; FTIR: Fourier-transforminfrared spectroscopy; BET: Brunauer-Emett-Teller; UV-Vis: Ultraviolet-Visible spectroscopy; ANOVA: Analysis of variance; df: Degrees of freedom; Std Dev: Standard deviation; Root MSE: Root-mean-square error; CV: Coefficient of variation.

Introduction

The significant chemical sector is the dye business, textile fibers, paper, leather, fur, wood, polymers, and elastomers can all be printed or dyed using dyes. Additionally, they serve as coloring additives in culinary and medicinal items as well as being used to produce paints, printing inks, and varnishes [1]. In the cosmetics sector, metal coloring (Anodized aluminum), photography (Sensitizers), biology

(Coloring of microscopic preparations), color indicators, and some are employed in medicines (Antiseptics, antimalarials, etc.) How to get rid of these dye leftovers has been the subject of extensive research in recent years. One of the dyes that is most frequently used on an industrial basis is basic yellow 28. The previous few decades have seen advancements in the treatment of industrial effluents, particularly textiles. Both the environment and human health are under danger from these effluents, which include this contaminant. Treatment of these substances is regarded as a contemporary global concern because of their toxicity, carcinogenicity, and mutagenicity [2].

The majority of this research has been focused on using biomaterials because of how well they work to cut down on environmental pollutants. These include flotation [3], precipitation [4], ion exchange [5], liquid-liquid extraction [6], photocatalysis [7], adsorption, etc. The latter is increasingly used due to its efficiency in the reduction of mineral micropollutants.

Adsorption intends to utilize adsorbents of organic origin, including activated carbon and bio-adsorbents [8, 9], as well as adsorbents of mineral origin, such as silicates [10], natural zeolites [11], natural clays [12]. Despite the fact that these adsorbents are exceedingly effective, their application is limited by their expensive cost [13]. For this reason, a number of researchers have concentrated their study on the creation of more affordable and alternative adsorbents.

The ability of calcium phosphate to act as an adsorbent and remove a variety of pollutants has recently been demonstrated by numerous studies [14-18]. In addition to having excellent biocompatibility and adsorption properties, nanocrystalline HAp $Ca_{10}(PO_4)_6(OH)_2$ is also considered to be a cost-effective adsorbent that can better retain the discharges of residual dyes like basic yellow 28 present in some textile industries. This biomaterial also has good cytocompatibility because it poses no environmental risk.

In this sense, we have focused our study on the treatment of water by adsorption on thesebiomaterials, for which we have chosen the basic yellow 28 in view of its permanent risks onthe environment and human health according to its toxicity even at low dose [2, 19].

The aim of this work is to study the influence of the variation of the important parameters that can impact on the adsorption yield (Initial concentrations of adsorbate, contact time between solute and adsorbate, and pH effect) in order to know the optimal conditions to obtain a maximum adsorption of basic yellow 28 by HAp and HAp-AMP according to the factorial plan method with the help of Design-Expert software.

Materials and Method

Materials

The synthesis of porous HAp and HAp-AMP was made by the wet process according to the method of neutralization of $Ca(OH)_2$ by $NH_4H_2PO_4$ in water medium. according to our procedurealready reported [13] in short. 14.82 g of $Ca(OH)_2$ were dissolved in 200 ml water (Solution 1). Reaction mixture was stirred for 90 min at room temperature. During the preparation of a mass of 13.80 g of $NH_4H_2PO_4$ dissolved in 100 ml water (Solution 2). The AMP grafting agent was added to that of solution 2 in variable proportions (0%, 2.5%, 5%, and 10%). Solution 2 was added rapidly to the calcium solution then stirred for 48 h. The final suspensions were filtered and washed with deionized water, then dried overnight at 100 °C. All used materials are nanoscale materials.

Characterization of HAp and HAp-AMP

Characterization of the products prepared at different grafting rates and dried at 100 °C by XRD, FTIR analysis, and BET method was performed according to our previously reported protocol [20].

XRD

The XRD analysis was performed on powder under ambient conditions of temperature and pressure in order to identify the different crystalline phases. The X-ray diffractometer used is a Philips PW131 equipped with a copper anticathode (λ = 1.5454Å) in the 2θ range from 10 to 90° and driven by a computer for data storage and processing.

FTIR

The IR spectra are recorded with a Fourier transform spectrometer VERTEX 70, the experiment showed that certain frequencies of vibration were characteristic to the presence of a chemical group in the studied molecule. The spectral range studied extends from 4000 cm^{-1} to 400 cm^{-1} with a resolution of 2 cm^{-1}

BET

The theory of BET aims to determine the specific surface of materials prepared with aMicromeritics ASAP2010 apparatus at 77 K.

Preparation and analysis of adsorbate solutions

The stock solution of basic yellow dye 28 is prepared by dissolving the required massof basic yellow in 1L of solution, without prior purification. The daughter solutions are prepared by successive dilutions of the stock solution to obtain 100 ml of solutions rangingfrom 5 mg/L to 100 mg/L. The adsorbate solutions before and after adsorption are analyzed by UV-Vis; UV-3100pc spectrophotometry at λ_{max} = 425 nm. The concentrations are then deduced from the Beer-Lambert law A = εℓC [21]. With: A:absorbance of the solution; ε: molar absorption coefficient of the substance ($L.mg^{-1}.cm^{-1}$); ℓ:optical path length (cm); and C: the concentration of the substance (mg/L). The calibrationis performed for concentrations of 5 to 20 mg/L.

Adsorption process of basic yellow 28 by apatites

The adsorption process of the dye on the apatite is followed by studies of various variables. In our work we choose to vary parameters which have a greater impact for the increase of adsorption rate this is why we worked on parameters (Initial concentration of the dye, pH, and contact time) are chosen as independent input variables and quantity of basic yellow 28 adsorbed as dependent response variable. The process of ad-

sorption of the dye onto the apatite is carried out by contacting 200 mg of the apatite under study in 10 ml of the desired 100 mg/L solution of basic yellow 28 at a temperature of 298 K. The mixture is stirred at 500 rpm. Which will be analyzed by UV-Vis spectroscopy. The adsorbed quantities (q_a) were calculated as the difference between the initial (C_0) and final (C_e) concentrations according to the following equation [12]:

$$q_a = \frac{C_0 - C_e}{m}. V$$

Where, qa: quantity of basic yellow 28 adsorbed per unit mass of adsorbent (mg/g), C_0: initial concentration of the dye (mg/L), Ce: residual concentration of basic yellow 28 at equilibrium (mg/L), V: volume of the solution (L), and m: mass of the adsorbent (g).

Design and optimization

Software developed by some researchers was used to analyze the impacts of varying experimental factors (Initial dye concentration studied, contact time, and pH) on basic yellow 28 dye by HAp-AMP 10% as a representative model. Because it has the highest adsorbed quantity. All experimental tests were performed according to Design-Expert 11 design matrix. Each factor has three levels, indicated by -1 for lowest, and +1 for highest (Table 1).

The matrix used in this study had 20 runs. All experiments were performed at room temperature. Table 2 shows the times at which the experimental samples were taken from the shaker.

Table 1: Variable levels for Design-Expert 11 software.

		-1	+1
Initial concentration (mg/L)	A	10	270
Contact time (min)	B	5	250
pH	C	4	12

Table 2: Plan matrix used in the present study.

Run	Factor 1: A (mg/L)	Factor 2: B (min)	Factor 3: C	Response: R Quantity Adsorbed (mg/g)
1	15.2	140.368	7.59096	8
2	15.2	140.368	7.59096	8
3	153	9.9	7.6	53
4	153	9.9	7.6	53
5	10	5	12	5
6	185.5	174.05	6.6	58
7	153	140.551	11.84	56
8	153	9.9	7.6	53
9	90.6	250	8.56	57
10	153	140.551	11.84	56
11	270	5	12	62
12	153	140.551	11.84	56
13	90.6	115.25	4	56.5
14	10	5	4	5
15	10	250	12	6.9
16	270	96.875	4	65
17	270	85.85	8.52	65
18	107.5	250	4	50
19	270	250	4	65
20	270	250	9	62

Results and Discussion

XRD

The XRD pattern of HAp is shown in figure 1. The lines of the XRD pattern have all been indexed in the hexagonal space group system $P6_{3/m}$ with crystal parameters of a = 9.432 Å and c = 6.883 Å.

We note that the XRD lines are relatively broad and that only the most intense lines are observed, whose intensity decreases as the grafting rate increases. XRD analysis showed that the incorporation of different levels of aminophosphonate leads to no alteration in apatite structure. The grafted apatites thus prepared are all weakly crystallized, so the low crystallinity of these apatites modified by AMP molecules enables us to identify the presence of small crystals. We note that modification of the HAp surface by AMP leads to no change in the crystalline phase of the HAp.

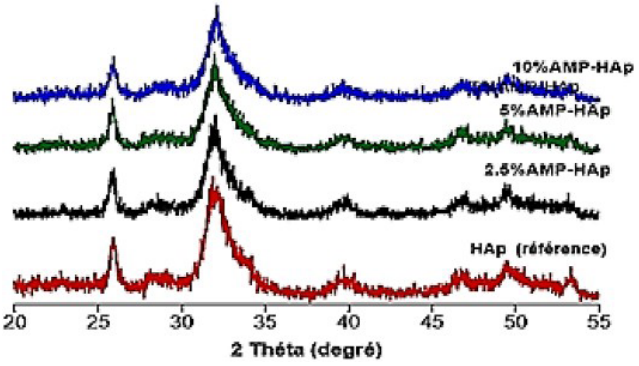

Figure 1: XRD patterns of prepared apatites.

FTIR analysis

Following the IR absorption spectra of the prepared apatites in figure 2. The IR absorption bands are shown in table 3, which reveals the absorption bands assigned to the PO_4^{3-} and OH^- groups of the apatite lattice.

The vibrational bands of the PO_4^{3-} groups of the apatite structure were detected by two absorption intervals located between 1100 - 900 cm^{-1} (In particular the bands located at 1090, 1030, and 962 cm^{-1}) and 600 - 500 cm^{-1} (Precisely those located at 603 and 565 cm^{-1}) with a slight shift towards high frequencies depending on the rate of grafting. This

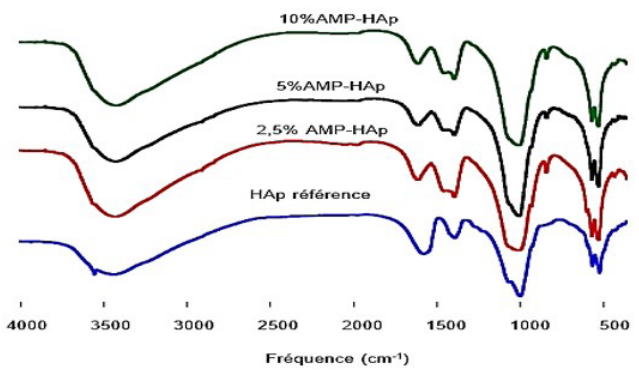

Figure 2: FTIR spectra of HAp-AMP apatites.

Table 3: FTIR absorption bands of prepared apatites.

Position of the absorption bands FTIR in cm^{-1}	Band intensities	Attributions
3560	Weak	OH-
1540	Weak	CO_3^{2-}
1480	Weak	CO_3^{2-}
1450	Weak	CO_3^{2-}
875	Weak	CO_3^{2-}
1090	Strong	PO_4^{3-}
1030	Very strong	PO_4^{3-}
962	Weak	PO_4^{3-}
630	Medium	OH^-
603	Strong	PO_4^{3-}
565	Strong	PO_4^{3-}

frequency shift is related to structural disorder and the nature of the organic (C-P-O) or inorganic (O-P-O) phosphorus bond. Other low intensity bands at 1540, 1480, 1450, 1416, and 875 cm^{-1} correspond unambiguously to the vibrational modes of CO_3^{2-} carbonates and other carbonyl groups. Some bands attributable to the vibration of the low intensity N(-CH_2-PO(OH)$_2$)$_3$ phosphonate oscillators are observed in conjunction with the increase in the rate of grafting, in particular the band around 1486 cm^{-1} which is due to the C-P vibrator, although that of N-C is covered by the bands associated with carbonates and phosphates. Moreover, the characteristic absorption bands of the vibrational frequencies of OH^- ions in the apatite lattice are located at 3560 and 630 cm^{-1}.

BET method

The aim of this method is to determine specific surface areas, volumes and pore diameters based on the principle of adsorption-desorption of nitrogen gas (Figure 3).

According to the results of the specific surface areas, pore volumes, and diameters of hybrid apatites compared with those of reference apatites (Table 4).

The specific surface area values of prepared apatites

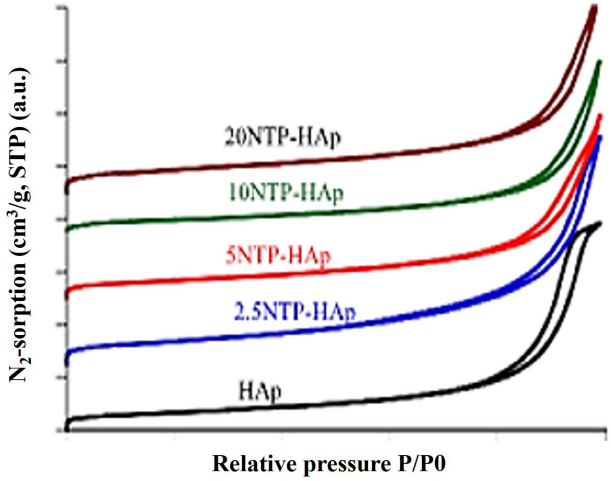

Figure 3: N_2-sorption isotherms for pure apatite (HAp) and organo-apatites powders.

Table 4: Specific surface areas, volumes, and pore diameters of hybrid apatites compared with reference apatite.

	HAp-AMP			
	0%	2.5%	5%	10%
SBET($m^2.g^{-1}$)	120	159	122	92
Dp (nm)	11	2.2 and 9.5	2.0 and 10.3	1.8 and 9.5

grafted with aminophosphonate decrease as a function of the grafting rate due to the structural arrangement of the aminophosphonate in the solid surface. which can be explained by the fact that the graft is voluminous [22].

Optimization of the adsorption process

Final equation in terms of coded factors

We can use a real equation of the actual factors to forecast the reaction to particular amounts of each factor.

The mathematical model coded with 20 factorial levels is indicated by:

Quantity Adsorbed = 10.2784 + 0.547856 * A + 0.0552019 * B - 2.76662 * C - 0.000132463 * A * B + 0.002251 * A * C - 0.00121747 * B * C - 0.00121478 * A2 - 1.03634e-05 * B + 0.125533 * C2

The above equation is used to establish the relative impact of the factors by comparing the coefficients of the factor. In this context. A has the greatest impact in this experiment because it has the largest coefficient, and we find that B is more influenced than C based on the comparison between their coefficients.

ANOVA

Further analysis of the elimination efficiency model equation can be performed using the ANOVA component of the software to check model significance and fit (Table 5). The p-values of the response model terms are less than 0.05 and the F-value is 27.34, respectively.

Fixed effects

The column labeled "df" indicates the degrees of freedom for each source. In response to the surface methodology, the total degrees of freedom are the same as the number of model coefficients added sequentially row by row. P-values less than 0.05 mean that the model expressions are significant and higher F values indicate that the model term has the most significant effect on the response function. In this case. A is a more significant model term [23].

Fit statistics

According to the statistics modeling. The different parameters and constants must be calculated such as [24]:

- The Std Dev and the square root of the residual mean square (RootMSE).
- In analysis the overall average of all response values (Mean).
- The CV is used to calculate the rate of the mean.

Table 5: Results of variance analysis (ANOVA).

Source	Sum of squares	df	Mean square	F-value	p-value	
Model	9794.75	9	1088.31	27.34	< 0.0001	
A-A	6799.62	1	6799.62	170.80	< 0.0001	
B-B	88.76	1	88.76	2.23	0.1663	
C-C	56.75	1	56.75	1.43	0.2601	
AB	24.78	1	24.78	0.6225	0.4484	
AC	7.47	1	7.47	0.1876	0.6741	
BC	1.85	1	1.85	0.0465	0.8335	
A^2	1673.40	1	1673.40	42.03	< 0.0001	**Significant**
B^2	0.0982	1	0.0982	0.0025	009614	
C^2	16.80	1	16.80	0.4219	0.5306	
Residual	398.10	10	39.81			
Lack of fit	398.10	5	79.62			
Pure error	0.0000	5	0.0000			
Cor total	10192.85	19				

- The R-squared used to represent the variation of the mean that has been attributed to amodel.
- The adjusted R-squared used to represent the variation and changes around the mean that was explained by the model, and which was adjusted for the number of terms in the model.

Table 6 shows that the predicted R^2 value of 0.7547 showed that the model was adequate and offered 75.47% variability in the prediction of removal efficiency during adsorption of basic yellow dye. The R^2 value of 0.9609 also implies that 96.09% of the variation in removal efficiency and adsorption capacity respectively can be attributed to the three factors considered. The difference between adjusted and predicted R^2 values was less than 20% [25].

This confirms that the response model is highly significant and indicates good agreement between experimental and predicted values of basic yellow removal efficiency.

The adequate response precision is greater than 4.0, implying that the model is in good agreement and highly significant [26].

Table 6: Modeling statistics.

Std Dev	6.31	**R^2**	0.9609
Mean	45.02	**Adjusted R^2**	0.9258
C.V. %	14.01	**Predicted R^2**	0.7547
		Adeq Precision	14.5759

Optimization of the adsorption process

The optimization of the different parameters used during the adsorption process the initial concentration of basic yellow 28, the contact time, and pH. This adsorption procedure is based on dissolution-precipitation of the prepared apatites. The response of this optimization was illustrated in figure 4 following the desirability function method of HAp-AMP 10%.

The optimum operating conditions for the adsorption of basic yellow 28 using grafted apatites were as follows: A- initial concentration of dye to 75 mg/L; B- contact time of 67 min, while pH has no significant impact on adsorption compared to other parameters. By setting these factors. We will obtain a quantity adsorbed of removal of the basic yellow 28 equal to 31.38 mg/g.

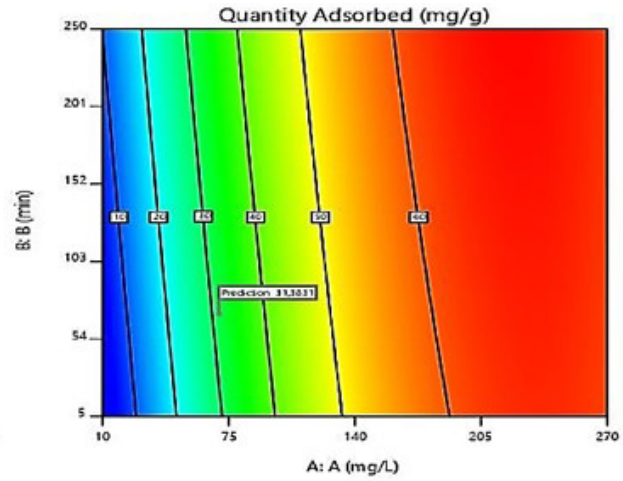

Figure 4: Optimized response.

Comparison of the apatite with other reported adsorbents

HAp-AMP 10% was compared with other materials according to the maximum adsorbed amount q_{max} of the basic yellow dye 28 to establish a comparative study and evaluate the adsorption performance (Table 7).

Table 7: Comparison of the maximum monolayer adsorption of basic yellow 28 onto various adsorbents.

Adsorbent	Adsorption capacity (q_{max})	Ref.
Our study (HAp-AMP 10%)	31.38 mg/g	This study
Watermelon seeds treated	57.88 mg/g	[27]
Conch shells	78.22 mg/g	[28]
New activated carbon (Wormwood)	357.142 mg/g	[29]
Amberlite XAD-4	8.7 - 14.9 mg/g	[30]
Coffee grounds	10 mg/g	[31]

In this study, the adsorption capacity of our HAp-AMP 10% adsorbent was not among the highest obtainable. But it represents a significant value compared with Amberlite XAD-4 and coffee grounds.

Conclusion

In this study, we have shown that it is possible to obtain HAp-AMP that could be good supports for the decontamination of industrial effluents, manifesting themselves with very fine particles that we have been able to prepare using a suitable method, having large specific surface areas compared with the reference. In addition. We concluded that the addition of AMP to the apatitic matrix inhibited apatite crystal growth. The main aim of this work was to demonstrate the influence of certain essential parameters on the retention capacity of our pollutant in the aqueous medium of basic yellow 28. It also aimed to identify the optimum conditions for maximum adsorption using an experimental design based on Design-Expert 11 software. As a result, we can say that the maximum removal of 31.38 mg/g of dye was obtained for an initial concentration of 75 mg/L and a contact time of 67 min and for pH has no significant impact on adsorption compared to other parameters. In this research, it could be concluded that HAp-AMP has a high potential for removing basic yellow dye 28 from aqueous media.

Acknowledgements

The authors would like to thank the Mohammed V University of Rabat, Morocco, for the financial support of this work.

Conflict of Interest

The authors declare that they have no conflict of interest.

References

1. Loukilia H, Mabroukic J, Anouzlab A, Kouzia Y, Younssia SA, et al. 2021. Pre-treated Moroccan natural clays: application to the wastewater treatment of textile industry. *Desalin Water Treat* 240: 124-136. https://doi.org/10.5004/dwt.2021.27644
2. Belal RM, Zayed MA, El-Sherif RM, Ghany NAA. 2021. Advanced electrochemical degradation of basic yellow 28 textile dye using IrO_2/Ti meshed electrode in different supporting electrolytes. *J Electroanal Chem* 882: 114979. https://doi.org/10.1016/j.jelechem.2021.114979
3. Malathy A, Manikandan V, Devanesan S, Farhat K, Priyadharsan A, et al. 2023. Development of biohybrid Ag_2CrO_4/rGO based nanocomposites with stable flotation properties as enhanced photocatalyst for sewage treatment and antibiotic-conjugated for antibacterial evaluation. *Int J Biol Macromol* 244: 125303. https://doi.org/10.1016/j.ijbiomac.2023.125303
4. De Castro MLFA, Abad MLB, Sumalinog DAG, Abarca RRM, Paoprasert P, et al. 2018. Adsorption of methylene blue dye and Cu(II) ions on EDTA-modified bentonite: isotherm, kinetic and thermodynamic studies. *Sustain Environ Res* 28(5): 197-205. https://doi.org/10.1016/j.serj.2018.04.001
5. Chang MF, Liu JC. 2007. Precipitation removal of fluoride from semiconductor wastewater. *J Environ Eng* 133(4): 419-425. https://doi.org/10.1061/(ASCE)0733-9372(2007)133:4(419)
6. Ma A, Abushaikha A, Allen SJ, McKay G. 2019. Ion exchange homogeneous surface diffusion modelling by binary site resin for the removal of nickel ions from wastewater in fixed beds. *Chem Eng J* 358: 1-10. https://doi.org/10.1016/j.cej.2018.09.135
7. Breil C, Vian MA, Zemb T, Kunz W, Chemat F. 2017. "Bligh and Dyer" and Folch methods for solid-liquid-liquid extraction of lipids from microorganisms. Comprehension of solvatation mechanisms and towards substitution with alternative solvents. *Int J Mol Sci* 18(4): 708. https://doi.org/10.3390/ijms18040708
8. Es-Sahbany H, Berradi M, Nkhili S, Hsissou R, Allaoui M, et al. 2019. Removal of heavy metals (nickel) contained in wastewater-models by the adsorption technique on natural clay. *Mater Today Proc* 13: 866-875. https://doi.org/10.1016/j.matpr.2019.04.050
9. Bali M, Tlili H. 2019. Removal of heavy metals from wastewater using infiltration-percolation process and adsorption on activated carbon. *Int J Environ Sci Technol* 16(1): 249-258. https://doi.org/10.1007/s13762-018-1663-5
10. Moghbeli MR, Khajeh A, Alikhani M. 2017. Nanosilica reinforced ion-exchange polyHIPE type membrane for removal of nickel ions: preparation, characterization and adsorption studies. *Chem Eng J* 309: 552-562. https://doi.org/10.1016/j.cej.2016.10.048
11. Radi S, El Abiad C, Moura NM, Faustino MA, Neves MGP. 2019. New hybrid adsorbent based on porphyrin functionalized silica for heavy metals removal: synthesis, characterization, isotherms, kinetics and thermodynamics studies. *J Hazard Mater* 370: 80-90. https://doi.org/10.1016/j.jhazmat.2017.10.058
12. Chen M, Nong S, Zhao Y, Riaz MS, Xiao Y, et al. 2020. Renewable P-type zeolite for superior absorption of heavy metals: isotherms, kinetics, and mechanism. *Sci Total Environ* 726: 138535. https://doi.org/10.1016/j.scitotenv.2020.138535
13. Saoiabi S, Achelhi K, Masse S, Saoiabi A, Laghzizil A, et al. 2013. Organo-apatites for lead removal from aqueous solutions: a comparison between carboxylic acid and aminophosphonate surface modification. *Colloids Surf A Physicochem Eng Aspects* 419: 180-185. https://doi.org/10.1016/j.colsurfa.2012.12.005
14. El Boujaady H, El Rhilassi A, Bennani-Ziatni M, El Hamri R, Taitai A, et al. 2011. Removal of a textile dye by adsorption on synthetic calcium phosphates. *Desalination* 275(1-3): 10-16. https://doi.org/10.1016/j.desal.2011.03.036
15. El Haddad M, Mamouni R, Saffaj N, Lazar S. 2012. Removal of a cationic dye–Basic Red 12–from aqueous solution by adsorption onto animal bone meal. *J Assoc Arab Univ Basic Appl Sci* 12(1): 48-54. https://doi.org/10.1016/j.jaubas.2012.04.003
16. Mourabet M, El Rhilassi A, El Boujaady H, Bennani-Ziatni M, El Hamri R, et al. 2012. Removal of fluoride from aqueous solution by adsorption on Apatitic tricalcium phosphate using Box–Behnken design and desirability function. *Appl Surf Sci* 258(10): 4402-4410. https://doi.org/10.1016/j.apsusc.2011.12.125
17. El Haddad M, Slimani R, Mamouni R, ElAntri S, Lazar S. 2013. Removal of two textile dyes from aqueous solutions onto calcined bones. *J Assoc Arab Univ Basic Appl Sci* 14(1): 51-59. https://doi.org/10.1016/j.jaubas.2013.03.002
18. Smičiklas ID, Lazić VM, Živković LS, Porobić SJ, Ahrenkiel SP, et al. 2019. Sorption of divalent heavy metal ions onto functionalized biogenic hydroxyapatite with caffeic acid and 3, 4-dihydroxybenzoic acid. *J Environ Sci Health Part A* 54(9): 899-905. https://doi.org/10.1080/10934529.2019.1606575
19. Cherif LC, Yahiaoui I, Aissani-Benissad F, Madi K, Benmehdi N, et al. 2014. Heat attachment method for the immobilization of TiO_2 on glass plates: application to photodegradation of basic yellow dye and optimization of operating parameters, using response surface methodology. *Ind Eng Chem Res* 53(10): 3813-3819. https://doi.org/10.1021/ie403970m
20. Saoiabi S, El Asri S, Laghzizil A, Saoiabi A, Ackerman JL, et al. 2012. Lead and zinc removal from aqueous solutions by aminotriphosphonate-modified converted natural phosphates. *Chem Eng J* 211: 233-239. https://doi.org/10.1016/j.cej.2012.09.017

21. Bouyarmane H, El Asri S, Rami A, Roux C, Mahly MA, et al. 2010. Pyridine and phenol removal using natural and synthetic apatites as low cost sorbents: influence of porosity and surface interactions. *J Hazard Mater* 181(1-3): 736-741. https://doi.org/10.1016/j.jhazmat.2010.05.074

22. da Silva OG, da Silva Filho EC, da Fonseca MG, Arakaki LN, Airoldi C. 2006. Hydroxyapatite organofunctionalized with silylating agents to heavy cation removal. *J Colloid Interface Sci* 302(2): 485-491. https://doi.org/10.1016/j.jcis.2006.07.010

23. Blume JD, Greevy RA, Welty VF, Smith JR, Dupont WD. 2019. An introduction to second-generation p-values. *Am Stat* 73(sup1): 157-167. https://doi.org/10.1080/00031305.2018.1537893

24. Roy P, Dey U, Chattoraj S, Mukhopadhyay D, Mondal NK. 2017. Modeling of the adsorptive removal of arsenic(III) using plant biomass: a bioremedial approach. *Appl Water Sci* 7: 1307-1321. https://doi.org/10.1007/s13201-015-0339-2

25. Rai A, Mohanty B, Bhargava R. 2016. Supercritical extraction of sunflower oil: a central composite design for extraction variables. *Food Chem* 192: 647-659. https://doi.org/10.1016/j.foodchem.2015.07.070

26. Bayuo J, Pelig-Ba KB, Abukari MA. 2019. Optimization of adsorption parameters for effective removal of lead(II) from aqueous solution. *Phys Chem Indian J* 14(1): 1-25.

27. Benkaddour S, El Ouahabi I, Hiyane H, Essoufy M, Driouich A, et al. 2020. Removal of basic yellow 28 by biosorption onto watermelon seeds, part I: the principal factors influencing by Plackett-Burman screening design. *Surf Interfaces* 21: 100732. https://doi.org/10.1016/j.surfin.2020.100732

28. El Ouahabi I, Slimani R, Benkaddour S, Hiyane H, Rhallabi N, et al. 2018. Adsorption of textile dye from aqueous solution onto a low cost conch shells. *J Mater Environ Sci* 9(7): 1987-1998.

29. Kenza A, Bensmaili A, Bouafia-Chergui S, Kadmi Y. 2020. New activated carbon from wormwood as efficient adsorbent of cationic dye in aqueous solution. *Iranian J Chem Chem Eng* 39(6): 137-148.

30. Yener J, Kopac T, Dogu G, Dogu T. 2006. Adsorption of basic yellow 28 from aqueous solutions with clinoptilolite and amberlite. *J Colloid Interface Sci* 294(2): 255-264. https://doi.org/10.1016/j.jcis.2005.07.040

31. Namane A, Mekarzia A, Benrachedi K, Belhaneche-Bensemra N, Hellal A. 2005. Determination of the adsorption capacity of activated carbon made from coffee grounds by chemical activation with $ZnCl_2$ and H_3PO_4. *J Hazard Mater* 119(1-3): 189-194. https://doi.org/10.1016/j.jhazmat.2004.12.006